

TRES Survey of Variable Diffuse Interstellar Bands

Charles J. Law,^{1*} Dan Milisavljevic,¹ Kyle N. Crabtree,² Sommer L. Johansen,²
 Daniel J. Patnaude,¹ Raffaella Margutti,³ Jerod T. Parrent,¹ Maria R. Drout,^{4,5}
 Nathan E. Sanders,¹ Robert P. Kirshner,^{1,6} David W. Latham¹

¹Harvard-Smithsonian Center for Astrophysics, 60 Garden St., Cambridge, MA 02138, USA

²Department of Chemistry, University of California, Davis, One Shields Ave., Davis, CA 95616, USA

³Center for Interdisciplinary Exploration and Research in Astrophysics (CIERA) and Department of Physics and Astrophysics, Northwestern University, Evanston, IL 60208, USA

⁴The Observatories of the Carnegie Institution for Science, 813 Santa Barbara St., Pasadena, CA 91101, USA

⁵Hubble, Carnegie-Dunlap Fellow

⁶Gordon and Betty Moore Foundation, 1661 Page Mill Road, Palo Alto, CA 94304, USA

Accepted XXX. Received YYY; in original form ZZZ

ABSTRACT

Diffuse interstellar bands (DIBs) are absorption features commonly observed in optical/near-infrared spectra of stars and thought to be associated with polyatomic molecules that comprise a significant reservoir of organic material in the universe. However, the central wavelengths of almost all DIBs do not correspond with electronic transitions of known atomic or molecular species and the specific physical nature of their carriers remains inconclusive despite decades of observational, theoretical, and experimental research. It is well established that DIB carriers are located in the interstellar medium, but the recent discovery of time-varying DIBs in the spectra of the extragalactic supernova SN 2012ap suggests that some may be created in massive star environments. Here we report evidence of short time-scale (~ 10 – 60 d) changes in DIB absorption line substructure toward 3 of 17 massive stars observed as part of a pathfinder survey of variable DIBs conducted with the 1.5-m Tillinghast telescope and Tillinghast Reflector Echelle Spectrograph (TRES) at Fred L. Whipple Observatory. The detections are made in high-resolution optical spectra ($R \sim 44000$) having signal-to-noise ratios of 5–15 around the 5797 and 6614 Å features, and are considered significant but requiring further investigation. We find that these changes are potentially consistent with interactions between stellar winds and DIB carriers in close proximity. Our findings motivate a larger survey to further characterize these variations and may establish a powerful new method for probing the poorly understood physical characteristics of DIB carriers.

Key words: astrochemistry – molecular processes – ISM: lines and bands – ISM: molecules – stars: mass-loss – stars: winds, outflows

1 INTRODUCTION

The nature of diffuse interstellar bands (DIBs) remains a long-standing problem in optical and near-infrared astronomy. DIBs, which represent over 500 absorption features, are generally narrow [full width at half-maximum (FWHM) < 1 Å] and weak (less than 5 per cent below continuum) with central wavelengths that do not correspond to known molecular or atomic species (Herbig 1995; Hobbs et al. 2009;

Geballe et al. 2011). The originating physical sources (or ‘carriers’) of the DIBs have remained a source of speculation and discussion since DIBs were first observed almost a century ago by Heger (1922).

Merrill (1934) originally suggested dust grains and molecules as possible carriers for the DIB features. These carriers remain the most plausible candidates after decades of observational, theoretical, and experimental work (see reviews by Herbig 1995, Fulara & Krelowski 2000, and Sarre 2006). Substantial observational evidence favors polyatomic, carbon-based molecular carriers. In particular, photo-UV-

* E-mail: claw@college.harvard.edu

resistant organic molecules (Douglas 1977), polycyclic aromatic hydrocarbons (PAHs) (Cox 2011), and fullerenes (Iglesias-Groth 2007) remain the most promising candidates. The recent unambiguous identification of C_{60}^+ as the carrier for two infrared DIB lines supports the notion that the carriers of DIBs are indeed organic molecules (Campbell et al. 2015).

Many observed properties of DIBs are best understood when interpreted as originating in carriers located in the interstellar medium (ISM). DIB features remain stationary in spectroscopic binaries (Merrill 1934), and extinction and Na I column density positively correlate with DIB intensity (Herbig 1995).

However, since the winds of massive stars are a principal source of replenishment for the ISM, it has been suspected that DIB carriers might also be present in circumstellar shells (CSs). To date, despite some evidence for possible DIB-CS associations in a narrow subset of mass-losing stars where temporal variations in DIB equivalent width, central wavelength, and substructure were observed (Le Bertre 1990; Le Bertre & Lequeux 1993), the majority of searches for carriers in CSs have proven unsuccessful or inconclusive (Le Bertre & Lequeux 1992; Sarre 2006; Luna et al. 2008).

The recent discovery of time-varying DIB features in optical spectra of the extragalactic Type Ic broad-lined supernova (SN) 2012ap calls into question the current assumption that all DIBs reside in the ISM (Milisavljevic et al. 2014). The equivalent width (EW) strength of DIB features observed toward SN 2012ap changed with time in a manner consistent with interaction between the SN and nearby DIB carrier(s) that possess high ionization potentials like those found in small cations or charged fullerenes. Milisavljevic et al. (2014) noted that archival data from two additional spectroscopically similar SNe also show evidence for temporal DIB variation, suggesting that a specific subset of SN progenitor stars may possess a CS environment enriched with DIB carriers.

Motivated by this recent discovery, we obtained high-resolution multi-epoch optical spectra of 17 massive stars as part of a pathfinder survey of variable DIBs. In this paper, we present the results from our survey, which finds evidence for substructural changes on short time-scales in the DIB absorption profiles towards three stars. We describe the observations, reduction of the raw spectral data, and the stellar sample selection in Section 2. In Section 3, we discuss the Gaussian fitting methods, determinations of errors, and data quality. We use these fitting methods and visual inspection to identify time-varying changes in DIB absorption features in Section 4. We discuss how these findings may be interpreted as interaction between strong stellar winds and the local carriers of DIBs in Section 5 and summarize our conclusions in Section 6.

2 OBSERVATIONS

2.1 Instrument and Data

High-resolution optical spectra were obtained with the 1.5-m Tillinghast telescope and Tillinghast Reflector Echelle Spectrograph (TRES) at Fred L. Whipple Observatory. TRES has a E2V 2K \times 4.5K CCD with 13.5- μ m pixels, and each

exposure provides nearly complete spectral coverage from 3850 to 9100 Å at a resolution of $R \approx 44\,000$ over the spectrograph's 51 orders (Szentgyorgyi & Furész 2007; Mink 2011). Multi-epoch observations were obtained between June 2013 and January 2014 for each star with co-added total exposure times ranging from 300 to 1800 s depending on the brightness of the source and observing conditions that were not always photometric. Time between observations ranged from \sim 10–60 d, were dependent on weather conditions and the TRES observing queue, and thus were not obtained at regular intervals. The typical spectral signal-to-noise (S/N) ratio in the region of DIB features was \gtrsim 5–15. A detailed list of observations is found in Table 1.

Raw spectra were reduced using the standard TRES data reduction pipeline (Mink 2011). The spectra were corrected for heliocentric velocity using the RVSAO software package in IRAF (Kurtz & Mink 1998). Continua of spectra were fit with Chebyshev functions and then continuum normalized using the `continuum` task. Example spectra of the 17 stars we observed around features of interest is shown in Fig. 1. Fits to stellar continua for three stars are shown in Fig. 2. Orders used for fitting ranged from 3rd to 15th depending on the complexity of the continuum. For each star, the lowest order fit over a broad range of wavelength in the relevant echelle order was chosen to mitigate any potential influence of other absorption features, which could skew the continuum fits. We have noted the few instances where the continua were particularly complex and difficult to fit and we discuss potential effects on our results in Section 5. We also experimented with higher order fits but found no significant differences in the resulting continuum fits or candidate DIB changes between epochs.

2.2 Sample Selection

We observed 17 stars at multiple epochs for the DIB variability survey. Candidate stars were selected from the literature based on whether pre-existing evidence of DIBs existed, and if they were mass-losing stars with enhanced O-rich or N-rich environments that could be correlated with DIB variability (as suggested by Le Bertre & Lequeux 1993). Wolf-Rayet (W–R) stars were favored since these are believed to be the progenitor stars of Type Ib/c supernovae like SN 2012ap (Gaskell et al. 1986; Milisavljevic et al. 2014). Spectral type, extinction, and further information for each source are found in Table 2.

3 METHODS AND ANALYSIS

3.1 Procedure

Before individual exposures were co-added, spectra were visually examined and found to be free of noise spikes around the features of interest, which could produce spurious line profile variations. The DIB features at 5780.6, 5797.1, and 6613.7 Å that were visible in all data were fit with Gaussian profiles using IRAF's `splot` task. Gaussian profiles are not true representations of DIB features but do provide a reasonable proxy by which to estimate their strength and central wavelength. Due to the poor response of the TRES instrument below 5000 Å, the DIB λ 4428 feature is not detected

Table 1. Summary of observations.

Star	RA(2000)	Dec(2000)	Date	UTC	Exposure Time(s)	Air Mass
HD 168607	18°21'15"	−16°22'32"	2013 June 2	09:02:04	360	1.49
			2013 July 31	05:33:41	450	1.50
HD 168625	18°21'19"	−16°22'26"	2013 June 2	09:10:20	360	1.50
			2013 July 31	05:44:40	450	1.52
HD 211853	22°18'45"	+56°07'33"	2013 Sept 11	08:31:40	300	1.21
			2013 Sept 19	07:22:19	300	1.15
			2013 Nov 14	04:42:23	300	1.25
			2013 Sept 25	04:39:53	300	1.11
HD 214419	22°36'53"	+56°54'21"	2013 Sept 11	08:59:27	300	1.23
			2013 Sept 19	07:30:01	300	1.15
			2013 Sept 23	03:30:26	360	1.21
			2013 Nov 14	04:49:42	300	1.23
AS314	18°39'26"	−13°50'47"	2013 June 2	08:48:29	660	1.44
			2013 July 3	10:03:39	1000	2.07
			2013 July 31	06:04:58	900	1.45
MT 59	20°31'10"	+41°31'53"	2013 Sept 11	06:46:29	600	1.14
			2013 Sept 19	04:21:34	600	1.02
			2013 Sept 26	03:30:03	800	1.02
			2013 Nov 26	01:45:53	600	1.14
MT 83	20°31'22"	+41°31'28"	2013 Sept 11	07:01:14	1200	1.18
			2013 Sept 19	04:37:22	1200	1.03
			2013 Sept 25	03:19:07	1200	1.02
			2013 Nov 26	02:10:27	1200	1.20
MT 145	20°31'49'	+41°28'26"	2013 Sept 19	06:00:58	1200	1.12
			2013 Nov 15	03:55:45	1200	1.42
MT 259	20°32'27"	+41°28'52"	2013 Sept 19	06:25:02	1200	1.17
			2013 Nov 15	04:18:45	1200	1.54
MT 457	20°33'14"	+41°20'21"	2013 Sept 19	06:48:15	1200	1.23
			2013 Nov 14	04:19:19	1200	1.52
MWC 314	19°21'33'	+14°52'56'	2013 June 02	08:18:15	1080	1.13
			2013 June 28	09:42:01	1200	1.12
			2013 July 24	08:21:08	900	1.15
WR 1	00°43'28"	+64°45'35"	2013 Sept 21	07:46:19	600	1.20
			2013 Sept 26	05:42:24	750	1.27
			2013 Nov 26	03:03:11	600	1.20
WR 2	01°05'23"	+60°25'18"	2013 Sept 11	10:05:30	1200	1.17
			2013 Sept 17	08:18:51	1200	1.14
			2013 Sept 21	08:00:49	1200	1.14
			2013 Sept 25	10:25:14	1350	1.25
			2013 Nov 26	03:23:14	1200	1.15
WR 3	01°38'56"	+58°09'23"	2014 Jan 11	03:07:16	600	1.16
			2014 Jan 21	02:48:53	600	1.19
WR 113	18°19'07"	−11°37'59"	2013 June 2	08:40:25	360	1.37
			2013 July 3	09:51:35	540	2.03
			2013 July 31	05:54:36	450	1.41
WR 124	19°11'30"	+16°51'38"	2013 June 2	07:52:29	1200	1.15
			2013 July 31	06:24:39	1200	1.04
WR 127	19°46'15"	+28°16'19"	2013 June 2	07:32:44	600	1.25
			2013 June 28	10:08:23	1800	1.07
			2013 July 27	07:52:31	1800	1.04

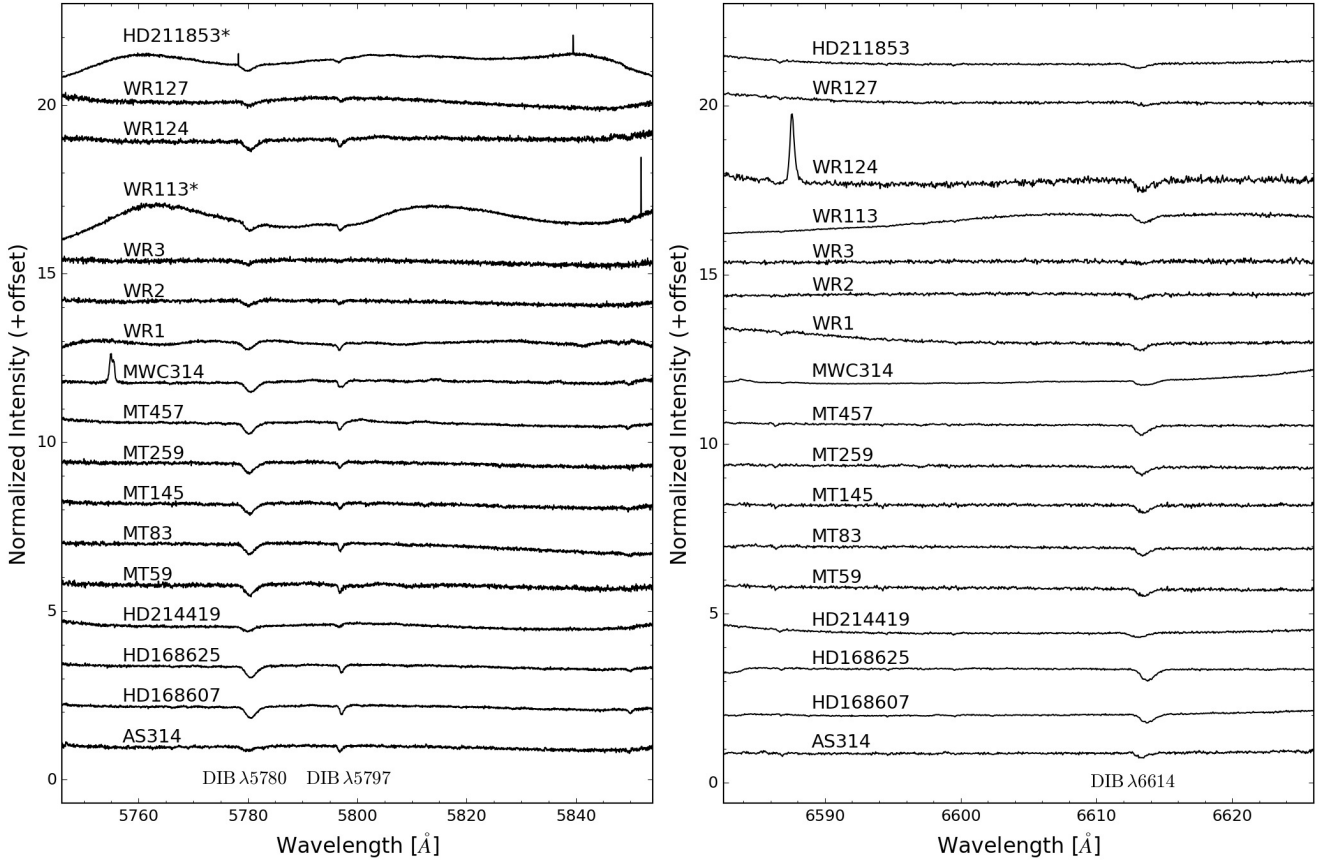


Figure 1. Representative spectra of the 17 stars observed in our survey. Two echelle orders spanning DIB features of interest at 5780, 5797, and 6614 Å are shown. The complete data set are available online. Spectra of HD211853 and WR113 marked with an asterisk (*) indicate instances where a 15th order Chebyshev function was insufficient to completely normalize the continuum.

in any of our observations. Some stars weakly exhibited the 6196.0 Å feature, but it could not be reliably measured. The feature at 6283.9 Å was also visible, but it was often contaminated by telluric absorption and at the edge of the order wavelength window. Thus, these features are not included in our reported analysis. The Na I feature, which provides a good measure of wavelength stability between epochs and thus tests for potential systematic errors, was fitted. We assumed 5889.950 and 5895.924 Å for the intrinsic wavelengths (Morton & Smith 1973). Multiple fittings for the equivalent width (EW) were done for each feature and averaged for each epoch, and the reported 1σ errors are given by the standard deviation of these fitting results. Radial velocities were derived by comparing the central wavelength of the Gaussian fittings to rest wavelengths of DIB features taken from the NASA DIBs catalogue (Jenniskens & Desert 1994).

3.2 Resolving DIB $\lambda 5797$ Substructure

We examined the well-studied DIB $\lambda 5797$ (cf. Sarre et al. 1995) to assess our ability to measure possible variation in DIB substructure. This DIB is known to have conspicuous substructural features believed to be associated with the rotational contours of gas-phase molecular carriers (Kerr et al. 1998). We were able to identify several characteristic sub-

structural components in this feature in all but two stars (AS 314 and WR 124). In these two outlying cases, we were limited by poor S/N around the feature. A representative spectrum showing the presence of this substructure is shown in Fig. 3. This exercise demonstrates that our observations with the TRES instrument permit careful investigation of potential changes in DIB substructure.

4 RESULTS

4.1 Resolved DIB Features

Our inspection of the data uncovered DIB variations in 3 of the 17 targets observed: WR 2, MT 59, and MT 145. The remaining 14 stars showed no measurable variations in DIB substructure, EW, or radial velocity. Of the three candidate stars we identify DIB variability, significant variations were seen in the 5797 and 6614 Å features, and marginal evidence for variation in the 5780 Å feature. Below we describe our results in detail.

4.2 WR 2

WR 2, also known as HD 6327, is a weak-lined Galactic WN2 star that is compact ($0.89 R_{\odot}$) and has a high temperature

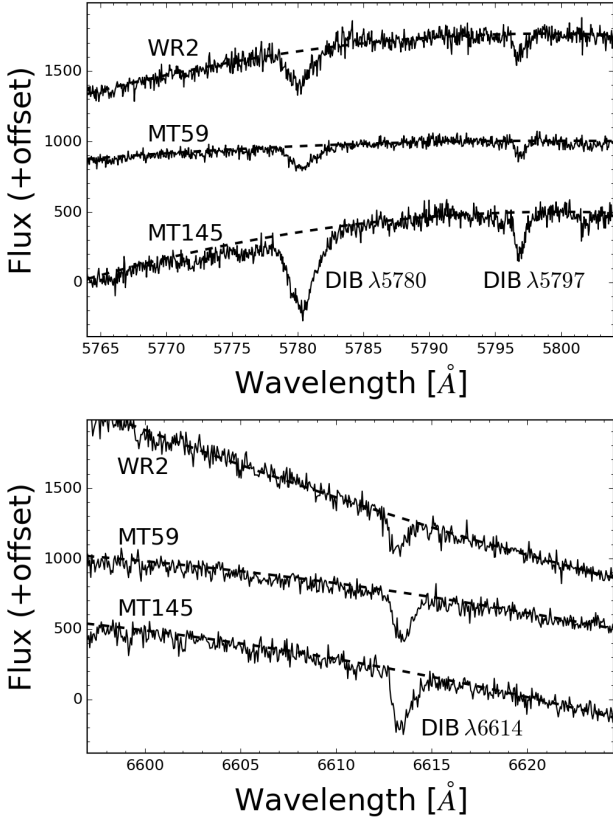


Figure 2. Example fits to stellar continua of WR 2, MT 59, and MT 145 used to normalize all spectra. For each epoch of these stars, the continuum was fitted with a 3rd order Chebyshev function to account for any continuum variability between observations. Fits to all other stars (see Table 1 for a complete listing) used also the Chebyshev function of order 3 to 15.

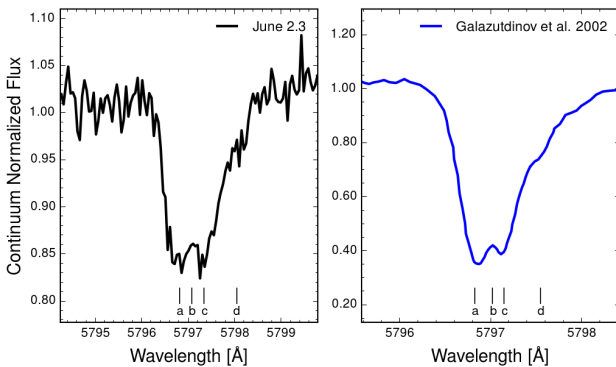


Figure 3. Spectral comparison of DIB $\lambda 5797$. The left plot shows a representative spectrum of MWC 314 taken on June 2, 2013 that shows several substructural features in DIB $\lambda 5797$. The right plot, a spectrum taken from Galazutdinov et al. (2002) using a spectrograph with resolution $R \sim 120,000$, shows comparable substructure to the spectral data of MWC 314. Four corresponding features have been labelled alphabetically in both plots.

Table 2. Properties of the stellar sample.

Star	Spectral Class	Other Designations	$E(B - V)$	Binarity	Reference
HD 168607	B9.4 Ia-0ep	V4029 Sgr, MWC 291	1.44	VB	1, 2
HD 168625	B5.6 Ia-0p	V4030 Sgr	1.33	VB	2
HD 211853	WN6o+06I	GP Cep	0.39	SB2	3, 11, 13
HD 214419	WN6+09II-Ib	CQ Cephei	0.41	SB1	4, 5, 11
AS 314	A0 Ia+	V452 Scuti	0.90	...	6
MWC 314	B3Ibe	V1429 Aquilae	1.45	SB1	7
WR 1	WN4-s	HD 4004	0.67	...	8, 14
WR 2*	WN2-w	HD 6327	0.44	VB	8, 14
WR 113	WC8d + 08-9IV	HD 168206, CV Ser	0.78	SB2	9, 11, 14
WR 124	WN8h	Hen 2-427	1.08	SB1	8, 14
WR 127	WN3 + 09.5V	HD 186943	0.27	SB2	8, 14
MT 59*	O8.5 V	Schulte 1	1.47	SB1	10, 12
MT 83	B1 I	Schulte 2	1.18	...	10, 12
MT 145*	O9.5 V	Schulte 20	1.11	SB1	10, 12
MT 259	B0.5 V	Schulte 21	1.00	...	10, 12
MT 457	O3 If	Schulte 7	1.45	...	10, 12

*Potential DIB variability detected.

References – (1) Chentsov & Gorda 2004; (2) Walborn & Fitzpatrick 2000; (3) Saurin et al. 2010; (4) Skinner et al. 2015; (5) Underhill et al. 1990; (6) Miroshnichenko et al. 2000; (7) Carmona et al. 2010; (8) Hamann et al. 2006; (9) David-Uraz et al. 2012; (10) Massey & Thompson 1991; (11) Ducati 2002; (12) Kobulnicky et al. 2014; (13) Panov & Seggewiss 1990; (14) van der Hucht 2001

(1.40×10^5 K). It exhibits rounded spectral profiles that are unique among Galactic W–R stars and do not match current models unless very rapid rotation (~ 1900 km s $^{-1}$) is assumed (Hamann et al. 2006). For each epoch, the continuum was fitted with a 3rd order Chebyshev function to account for any continuum variability between observations. Examples of the continuum fits are shown in Fig. 2.

In Fig. 4, we plot the results of our measurements, and show spectra of select epochs around the DIB $\lambda 5797$ feature illustrating how changes in radial velocity coupled with modest EW variations are the consequence of substructural changes within the DIB $\lambda 5797$ feature. The radial velocity variations are seen at the $\approx 3\sigma$ level. The detection, disappearance, and then slight re-emergence of a substructural feature on the blue wing of the DIB as well as a deeper, sharply peaked feature in the blue side of the minimum of the absorption trough can be seen (labelled ‘a’ and ‘b’, respectively in Fig. 4). We also detect the appearance of a shallow dip in the right wing of DIB $\lambda 5797$ (labelled ‘c’ in Fig. 4) between September 17.3 and November 26.1. The DIBs at 5780 and 6614 Å show no measurable changes EW, and a marginal decrease in radial velocity. Na I remains unchanged throughout all epochs.

4.3 MT 59

MT 59 is a massive O-type star located in Cygnus OB2 (Massey & Thompson 1991; Wright et al. 2015). For each epoch, the continuum was fitted with a 3rd order Chebyshev function to account for any continuum variability between observations (see Fig. 2). In Fig. 5 we plot our measurements of changes in the DIB $\lambda 5780$, $\lambda 5797$, and $\lambda 6614$ features of MT 59, as well as select epochs of spectra enlarged around DIB $\lambda 5797$ and $\lambda 6614$ features that exhibit the most conspicuous changes. Between September 26.1 and November 26.1, a prominent substructural change is seen as well as a $\gtrsim 3\sigma$ variation in the radial velocity of DIB $\lambda 6614$. The red wing of the DIB spanning 5797.6 to 5798.6 Å (labelled ‘a’ in Fig. 5 and labelled ‘d’ in Fig. 3) decreases in strength. A marginal

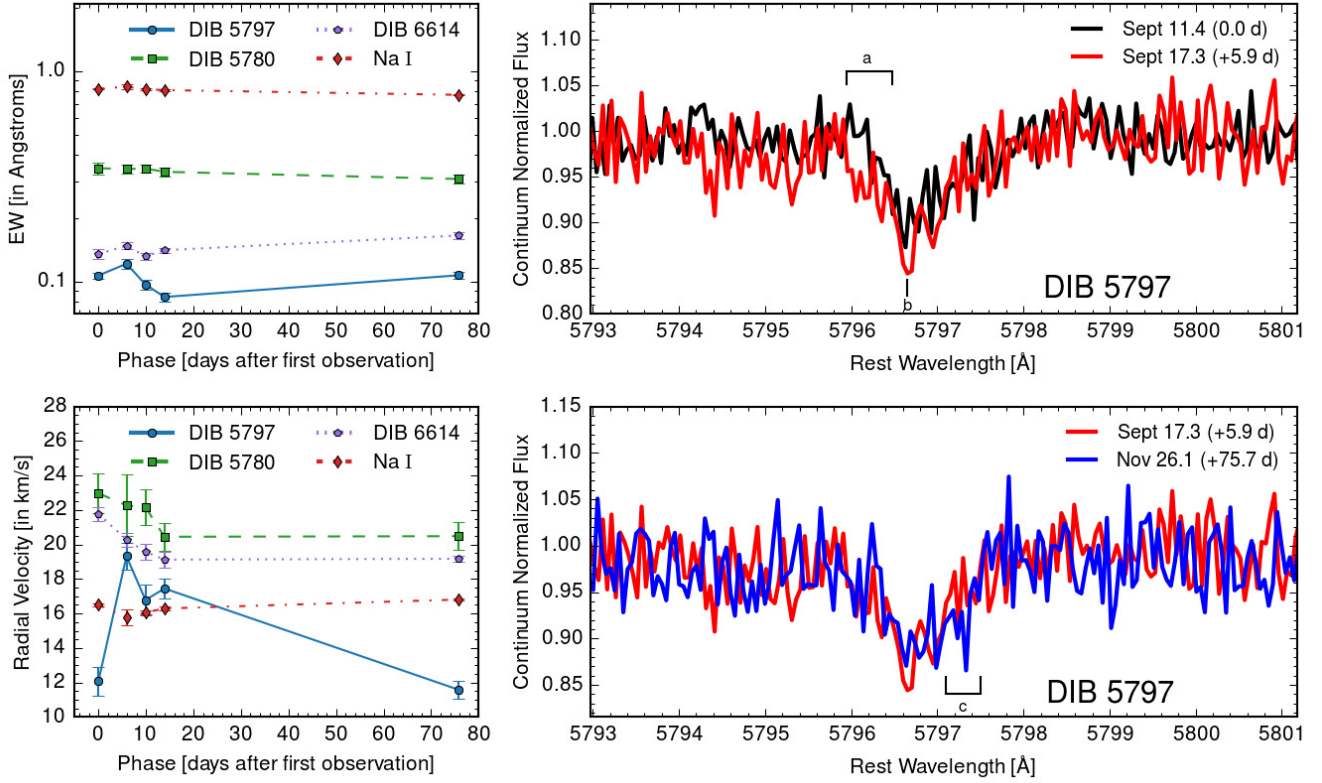


Figure 4. Left: EW and radial velocity measurements for WR 2. The features DIB λ 5797, DIB λ 5780, DIB λ 6614, and Na I are shown for all measured epochs. Note that the EW and radial velocity of Na I remains stationary. Error bars represent 1σ uncertainties. Right: Multi-epoch comparison of raw spectra for DIB λ 5797 feature of WR 2. The plots step through selected epochs in which there is evidence for DIB substructural changes and the relevant wavelength regions are labelled alphabetically.

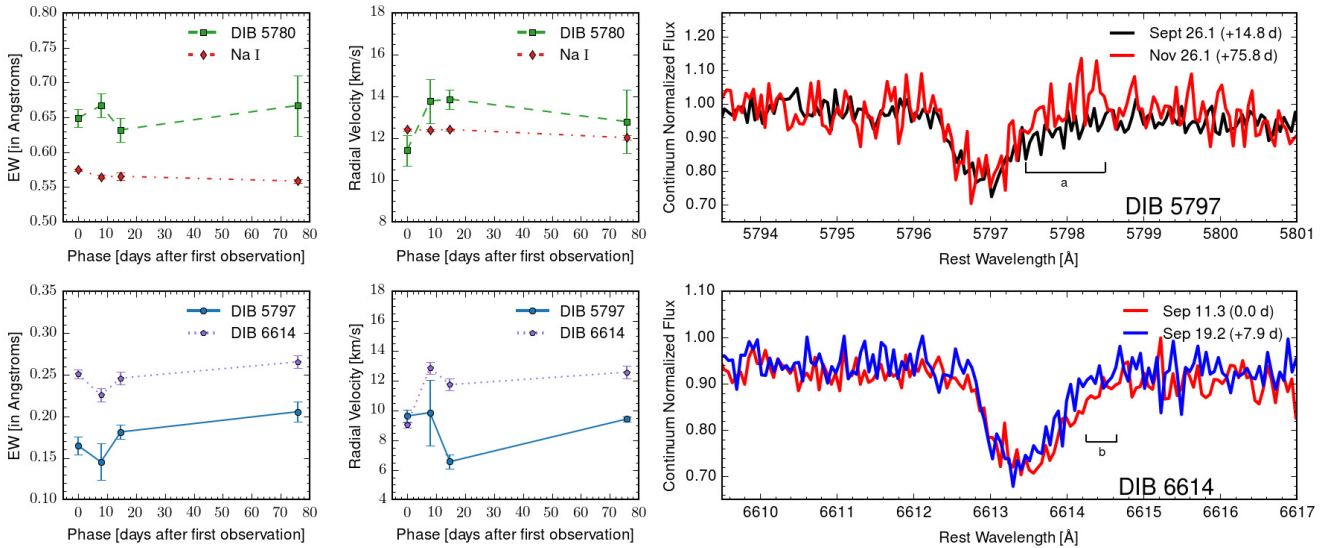


Figure 5. Left: EW and radial velocity measurements for MT 59. The features DIB λ 5780, DIB λ 5797, DIB λ 6614, and Na I are shown for all measured epochs. For clarity, DIB λ 5780 is shown in the top row and DIB λ 5797 is presented in the bottom row. Note that the EW and radial velocity of Na I remains stationary. Error bars represent 1σ uncertainties. Right: Multi-epoch comparison of raw spectra for DIB λ 5797 and λ 6614 features of MT 59. The plots step through selected epochs in which there is evidence for DIB substructural changes and the relevant wavelength regions are labelled alphabetically.

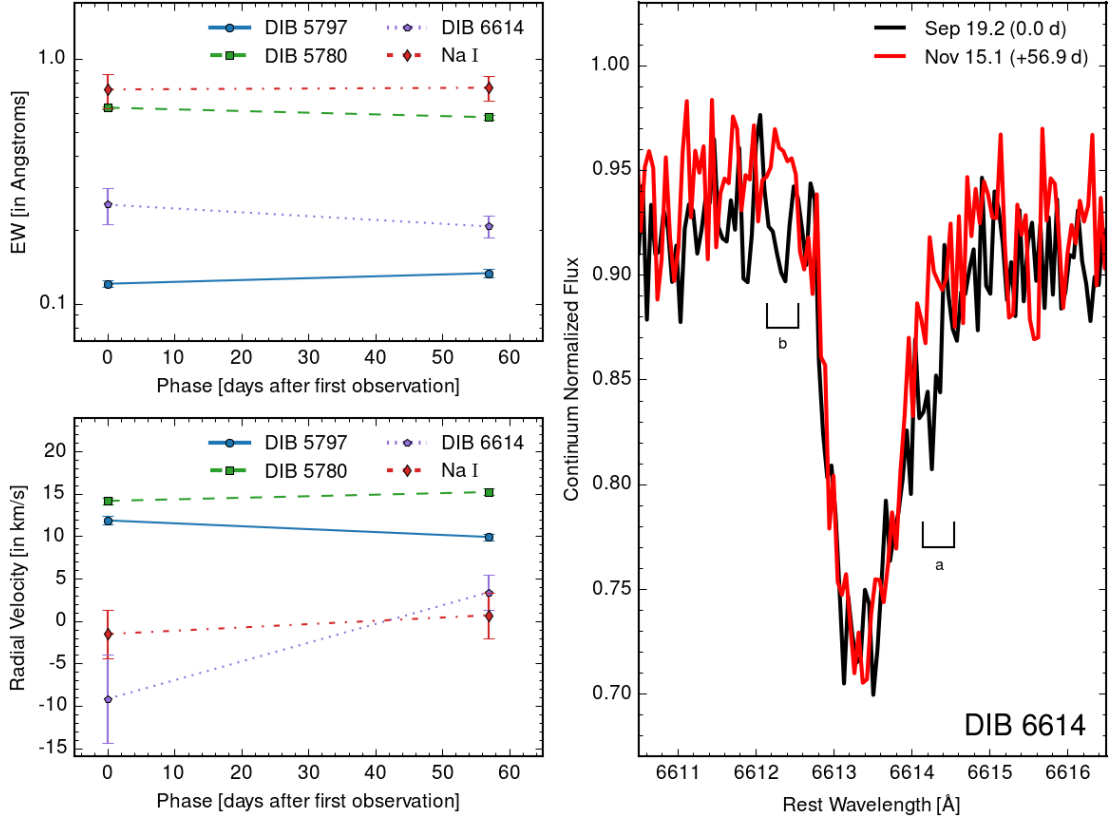


Figure 6. Left: EW and radial velocity measurements for MT 145. The features DIB λ 5780, DIB λ 5797, DIB λ 6614, and Na I are shown for all measured epochs. Note that the EW and radial velocity of Na I remains stationary. Error bars represent 1σ uncertainties. Right: Multi-epoch comparison of raw spectra for DIB λ 6614 feature of MT 145. The plots step through the two available epochs in which there is evidence for changes in DIB substructure. The one relevant wavelength region is labelled.

decrease is also detected in the red wing of the DIB λ 6614 feature (labelled ‘b’ in Fig. 5) between September 11.3 and September 19.2. The DIB at 5780 Å shows no measurable changes in EW and negligible variations in radial velocity. Na I remains unchanged throughout all epochs.

4.4 MT 145

MT 145 is also a massive O-type star located in Cygnus OB2 (Massey & Thompson 1991; Wright et al. 2015). For each epoch, the continuum was fitted with a 3rd order Chebyshev function to account for any continuum variability between observations. Measurements of changes in its DIB λ 5780, λ 5797, and λ 6614 features are shown in Fig. 6, as well as spectra enlarged around DIB λ 6614 that exhibited the most conspicuous change. From September 19.2 to November 15.1, we detect an increase in a broad feature on the red and left wings of DIB λ 6614 (labelled ‘a’ and ‘b’ in Fig. 6, respectively). The DIBs at 5780 and 5797 Å exhibit no measurable changes in EW and only minor radial velocity changes. Na I remains unchanged throughout all epochs.

4.5 Robustness of Our Detections

In order to quantify the significance of our DIB temporal variation detections, we compared the average flux excess

(or deficiency) as measured by the difference between our spectra and continuum fits. The difference between observation and continuum fit was made in two directly adjacent 2.5 Å windows centered on the DIB feature. An advantage of this method is that it incorporates the relatively broad spectral width of the observed variations that are much larger than narrow pixel-to-pixel noise fluctuations. For instance, the substructural feature labeled ‘a’ in Fig. 4 is not substantially larger in flux than a noise feature at about 5794.3 Å but ‘a’ is distributed over ≈ 0.6 Å while the noise feature of similar depth happens only over ~ 0.2 Å.

For profiles consistent with no temporal change, no substantial flux excess is expected relative to that of the continuum, which is set by the root-mean-square fluctuations. However, for the broad changes seen toward the wings of DIBs profiles, which represent the majority of our candidate changes, we typically observe $\sim 1.5\times$ flux differential between the DIB features and the continuum. The variation observed in WR 2 in DIB λ 5797 between Sept. 11.4 and 17.3 has a particularly large flux excess that is factor of $\sim 24\times$ larger than the continuum. We note that this method is not sensitive to changes in the form of narrow spectral spikes, e.g., WR 2, ‘c’ for DIB λ 5797, that may in fact be attributable to noise in the extracted spectrum.

Variable DIB features detected in WR 2 and MT 59 pass our flux excess test and support the view that the observed

changes are intrinsic to the profile and not artificial. The candidate detections in MT 145, however, do not pass this test and thus we are less confident in their reality.

5 DISCUSSION

5.1 Variable Diffuse Interstellar Bands

We observe measurable changes in absorption line substructure around the DIB $\lambda 5797$ and $\lambda 6614$ features over relatively short time-scales ($t < 60$ d). These changes are unlike normal DIB profiles that are static and remain unchanged, even after > 40 yr of observing (Herbig 1995). They are also unlike the changes observed in DIB absorptions toward SN 2012ap (Milisavljevic et al. 2014). In that case, the evolution was observed as pronounced changes in EW absorption strengths, as opposed to modifications of profile substructure that we observe in WR 2, MT 59, and possibly MT 145.

Robust fitting of stellar continua is a known challenge in DIB profile analyses (see, e.g., Galazutdinov et al. 2008b), and could potentially contribute to changes in DIB profile structure like those seen in our spectra. We are unable to conclusively rule out a changing continuum between observational epochs. However, no conspicuous changes in the continua that have been fit with 3rd order Chebyshev polynomials between epochs is observed. Thus, we interpret these changes to be intrinsic to the DIB profiles and not due to changes in the stellar continua.

Spectra of increasing quality and resolution obtained over the past two decades have hinted at variations in the profiles of individual DIBs along different sight lines. In some cases, the observed profiles reflect the complex structure of the ISM made up of multiple clouds moving at a range of velocities (e.g., Herbig & Soderblom 1982; Weselak et al. 2010). However, not all differences in profile shapes observed along different sight lines can be accounted for this way. Moreover, defining characteristics of these profile shape differences resemble the DIB variations reported here.

For example, Krelowski et al. (1997) observed the DIB $\lambda 5797$ feature at $R \approx 60\,000$ using the McDonald Observatory echelle spectrograph toward several ζ , ρ , and σ -type sources (see their paper for a more careful definition of these terms), and observed slight differences in the fine structure on the redward side. These subtle substructure variations have been repeatedly documented in a series of high-resolution surveys of sight lines probing only a single cloud by Galazutdinov et al. (2002), Galazutdinov et al. (2008b) and Galazutdinov et al. (2008a), which confirmed that the variations in profile are intrinsic to the carrier, and not due to Doppler effects.

Dahlstrom et al. (2013) and Oka et al. (2013) have reported observations of several DIBs ($\lambda 5780$, $\lambda 5797$, and $\lambda 6614$) that show very prominent extended tails toward the red (ETRs) in Her 36, suggesting that the carriers are polar molecules that are being radiatively pumped by nearby dust emission, leading to elevated rotational temperatures. A comparison of their spectra toward Her 36 and 9 Sgr (which shows no ETR), shown in fig. 3 of Oka et al. (2013), bears striking resemblance to the comparison of our spectra toward MT 59 taken on September 26 and November 26, respectively (Fig. 5). Likewise, the differences observed in the extended sidebands of the DIB $\lambda 6614$ profiles towards HD

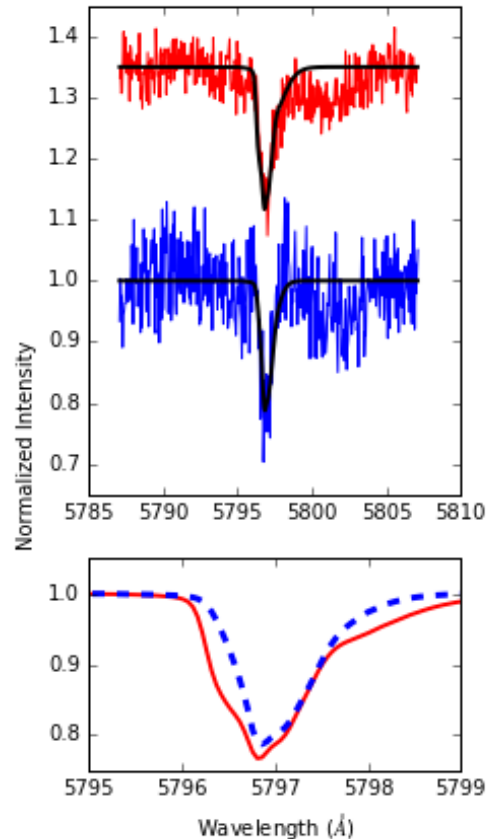


Figure 7. Model fits to the DIB $\lambda 5797$ profile of MT 59 using the models of Huang & Oka (2015). The top panel shows the observational data and best model for September 26 (top, Model A, 60% 45 K) and November 26 (bottom, Model A, 50% 20 K). The bottom panel contains a closer view of the differences between the models.

179406 and HD 147889 presented in Marshall et al. (2015) and explained in terms of vibrational hot bands, are similar to the two epochs of MT 145 presented here (Fig. 6).

Searches for time-varying DIBs were conducted toward κ Velorum by Smith et al. (2013). Known atomic absorption lines changed over time but DIB features did not, indicating that DIBs do not necessarily follow the same trends as atomic transitions. These results are not inconsistent with our own findings. Whereas the DIBs investigated in Smith et al. (2013) were primarily interstellar in origin, we propose that the variations we observe must result from circumstellar DIB carriers interacting with the massive star winds.

These results all support the notion that DIB absorption profiles can exhibit substructure that is sensitive to the environmental conditions in which carrier molecules reside. In the next section we test the plausibility of this hypothesis by modeling the variable DIB $\lambda 5797$ profile of MT 59 assuming changes in temperature.

5.2 DIB $\lambda 5797$

DIB $\lambda 5797$ is a strong, well-studied feature whose profile resembles the rotational fine structure associated with a molecular rovibronic transition, as best illustrated by the

$R \approx 600\,000$ spectrum of Sarre et al. (1995) acquired toward μ Sgr using the Ultra-High-Resolution Facility at the Anglo-Australian Telescope (Diego et al. 1995). Our observations of MT 59 may suggest that at least some of the molecular carriers of DIB $\lambda 5797$ are experiencing time-varying internal excitation due to an interaction with the star. If this is true, the nature of the interaction may help shed light on the molecular carrier. However, since the carrier is unknown, it is difficult to reliably interpret the changes in the profile.

Several attempts have been made to model the fine structure of DIBs $\lambda 5797$ in terms of specific types of spectroscopic transitions of free molecules. Kerr et al. (1998) performed a contour modeling study based on a perpendicular transition in a planar (oblate) symmetric top molecule, but were unable to achieve a satisfactory match. Oka et al. (2013) modeled the ETRs as a ${}^2\Pi \leftarrow {}^2\Sigma$ perpendicular band in a linear molecule. Although their model reproduced the ETRs, it did not match the fine structure at the top of the band. A later model of DIB $\lambda 5797$ in a more typical source by Huang & Oka (2015), based on a ${}^2\Pi \leftarrow {}^2\Pi$ parallel transition in a linear radical with 5–7 heavy atoms, was able to generally reproduce the ETRs with some success assuming a 2 component mixture with different rotational temperatures in order to approximate a higher level of rotational excitation due to radiative pumping. The same model can also generally account for the structure in more typical sources that do not display the ETRs by assuming a rotational temperature of 2.73 K appropriate for a polar molecule in a low-density environment.

The limited resolution of our spectra and low S/N ≈ 5 –15 of DIB $\lambda 5797$ in our data preclude a detailed quantitative analysis of the profile variations. However, if we adopt the interpretation of Huang & Oka (2015), we might ascribe the increase in absorption on the red side of this feature in MT 59 (Fig. 5) to a time-dependent change in the excitation temperature of a portion of the DIB carriers due to an interaction with the massive star. Such an effect could occur in one of two ways: 1) if the radiation field of the star changes with time, a portion of the carriers could be radiatively pumped into higher internal states, ultimately leading to a higher rotational excitation temperature, or 2) some of the DIB carriers may experience an interaction with a clumpy mass-loss wind, leading to an increased collision rate that increases the excitation temperature of the carrier’s rotational distribution above 2.73 K.

We inspected the stellar features of our candidate stars for conspicuous and unexplainable changes coincident with changes observed in the DIB features but were unable to find any. Specifically, the fine structure of the emission line profiles of WR 2 did not exhibit any measurable changes between epochs, and the temporal variation of H and He absorption features of MT 59 and MT 145 (most conspicuous being H α and He I $\lambda 5876$) was consistent with their nature as single-lined binary systems (Kobulnicky et al. 2014). Thus we have no direct evidence that the stellar radiation field exhibited significant changes during the observational period. However, massive stars are known to exhibit temporally varying mass-loss winds on these time-scales (Moffat et al. 1988; Tuthill et al. 1999), so the latter interpretation is attractive.

We attempted to reproduce the DIB $\lambda 5797$ profiles of

MT 59 using the program PGOPHER¹, in combination with the models of Huang & Oka (2015). For each model (A, B, and C), molecular spectra were simulated at temperatures ranging from the background radiative temperature (2.73 K) up to 60 K. We then constructed synthetic spectra from two-component mixtures consisting of a 2.73 K component with variable amounts (0–100%) of a second, higher temperature component for each original model from Huang & Oka (2015) in order to simulate additional rotational excitation. Comparing all these models to the MT 59 September 26 data, the best match involved a $\sim 50/50$ mixture of a 40–60 K and a 2.73 K spectrum derived from Model A, while the MT 59 November 26 was best fit by a 50/50 mixture whose warmer component was 20 K (Figure 7). Model C showed qualitatively similar results, while model B was found to be a poor fit in general to the September 26 data. While higher SNR spectra will be required to derive any firm conclusions, our preliminary analysis supports the notion that a change in the rotational excitation of the DIB carrier population could explain the profile changes tentatively observed between epochs.

6 CONCLUSIONS

We have presented the results of a pathfinder survey of 17 massive stars conducted with the TRES high resolution spectrograph that looked for changes in DIB absorption features over multiple epochs. We find evidence for time-varying changes in three stars WR 2, MT 59, and MT 145 in the substructure of the DIB $\lambda 5797$ and $\lambda 6614$ features over relatively short time-scales ($t < 60$ d). The changes are most pronounced along the wings of the profiles. Sharp and narrow features (< 0.2 Å) are also seen to come and go, but their reality is less secure. The changes in WR 2 and MT 59 pass our flux excess test and are our leading candidate detections, whereas the changes in MT 145 fail this test and have a greater chance of being due to noise in the extracted spectrum.

We have proposed that the short-term DIB variability we observe may be the consequence of carrier molecules interacting with the winds of nearby host stars. We do not find any correlation between DIB changes and changes in stellar emission/absorption features to support this hypothesis. However, using the models of Huang & Oka (2015), we find it plausible that changes in rotational excitation of the carrier molecules could be responsible for the observed changes in DIB substructure observed in our data between epochs.

Our results imply that carrier molecules responsible for the DIB absorption variability must be located in close proximity to massive stars (i.e., within their circumstellar shells). This conclusion runs counter to numerous studies that support the view that DIBs are a static large-scale phenomenon not located in circumstellar environments (Seab 1995; Luna et al. 2008; Cox 2011). However, theoretical and observational evidence increasingly favor the notion that DIB carriers are large gas phase molecules (e.g. PAHs or fullerenes)

¹ <http://pgopher.chm.bris.ac.uk/>

that could very well be present in circumstellar shells and detectable under specific circumstances.

Notably, recent work suggests that the mere presence of carbon-rich space environments may not be enough to detect DIB carrier material, and that proximity to a strong source of ionizing photons may be an important factor in producing enhanced DIB absorptions (see, e.g., Milisavljevic et al. 2014; and Díaz-Luis et al. 2015 who report evidence of unusually intense DIB $\lambda 4428$ and DIB $\lambda 5780$ features in fullerene planetary nebulae). Furthermore, if mass loss is concentrated along circumstellar discs, then the ability to observe DIB variations may also be related to line of sight effects. Taken together, observing DIBs in circumstellar environments may be relatively difficult and the instances rare given the numerous conditions that need to be satisfied in order for them to be detectable.

Our survey demonstrates the need for instrumental stability, appropriate observing cadence, high spectral resolution, and superior S/N in order to successfully detect DIB profile changes. A future survey could test our claims of DIB variability and improve on our work by observing more stars with spectra of S/N $\gtrsim 100$. Observations made at evenly spaced intervals matching orbital periods of known binary systems could look for repeated DIB variability correlated with stellar absorption and/or emission features. Broader wavelength coverage could potentially identify new families of time-varying DIBs and probe the DIB $\lambda 4428$ feature, which was not studied in this investigation but exhibited the most conspicuous changes in spectra observed from SN 2012ap. Using information about the environments of these stars (e.g. temperature and ionizing radiation) in combination with contour models, the temporal variations observed in these DIBs may provide a new way to probe the physical properties of their carriers.

ACKNOWLEDGEMENTS

We thank I. Crawford who provided many helpful comments and suggestions that improved the quality and presentation of this paper. E. Berger kindly provided helpful comments on an earlier draft of the paper. The observations reported in this paper were obtained at the Fred L. Whipple Observatory, which is operated by the Smithsonian Astrophysical Observatory. We thank L. Buchhave, G. Esquerdo, P. Berlind, M. Calkins, and J. Mink for help planning, obtaining, and reducing these data. C. L. thanks the Harvard College Program for Research in Science and Engineering that provided financial support for this work, as well as the Universities Space Research Association for additional support through the Frederick Tarantino Memorial Scholarship Award.

REFERENCES

Campbell E. K., Holz M., Gerlich D., Maier J. P., 2015, *Nature*, 523, 322
 Carmona A., van den Ancker M. E., Audard M., Henning T., Setiawan J., Rodmann J., 2010, *A&A*, 517, A67
 Chentsov E. L., Gorda E. S., 2004, *Astronomy Letters*, 30, 461

Cox N. L. J., 2011, in Joblin C., Tielens A. G. G. M., eds, *EAS Publications Series Vol. 46*, EAS Publications Series. pp 349–354, doi:10.1051/eas/1146036
 Dahlstrom J., et al., 2013, *Astrophys. J.*, 773, 41
 David-Uraz A., et al., 2012, *MNRAS*, 426, 1720
 Díaz-Luis J. J., García-Hernández D. A., Kameswara Rao N., Manchado A., Cataldo F., 2015, *A&A*, 573, A97
 Diego F., et al., 1995, *MNRAS*, 272, 323
 Douglas A. E., 1977, *Nature*, 269, 130
 Ducati J. R., 2002, *VizieR Online Data Catalog*, 2237
 Fulara J., Krelowski J., 2000, *New Astron. Rev.*, 44, 581
 Galazutdinov G., Stachowska W., Musaev F., Moutou C., Lo Curto G., Krelowski J., 2002, *A&A*, 396, 987
 Galazutdinov G. A., Lo Curto G., Krelowski J., 2008a, *MNRAS*, 386, 2003
 Galazutdinov G. A., LoCurto G., Krelowski J., 2008b, *ApJ*, 682, 1076
 Gaskell C. M., Cappellaro E., Dinerstein H. L., Garnett D. R., Harkness R. P., Wheeler J. C., 1986, *ApJ*, 306, L77
 Geballe T. R., Najarro F., Figer D. F., Schlegelmilch B. W., de La Fuente D., 2011, *Nature*, 479, 200
 Hamann W.-R., Gräfener G., Liermann A., 2006, *A&A*, 457, 1015
 Heger M. L., 1922, *Lick Observatory Bulletin*, 10, 141
 Herbig G. H., 1995, *ARA&A*, 33, 19
 Herbig G. H., Soderblom D. R., 1982, *ApJ*, 252, 610
 Hobbs L. M., et al., 2009, *ApJ*, 705, 32
 Huang J., Oka T., 2015, *Mol. Phys.*, 8976, 1
 Iglesias-Groth S., 2007, *ApJ*, 661, L167
 Jenniskens P., Desert F.-X., 1994, *A&AS*, 106
 Kerr T. H., Hibbins R. E., Fossey S. J., Miles J. R., Sarre P. J., 1998, *ApJ*, 495, 941
 Kobulnicky H. A., et al., 2014, *ApJS*, 213, 34
 Krelowski J., Schmidt M., Snow T. P., 1997, *Publ. Astron. Soc. Pacific*, 109, 1135
 Kurtz M. J., Mink D. J., 1998, *PASP*, 110, 934
 Le Bertre T., 1990, *The Messenger*, 59, 46
 Le Bertre T., Lequeux J., 1992, *A&A*, 255, 288
 Le Bertre T., Lequeux J., 1993, *A&A*, 274, 909
 Luna R., Cox N. L. J., Satorre M. A., García Hernández D. A., Suárez O., García Lario P., 2008, *A&A*, 480, 133
 Marshall C. C. M., Krelowski J., Sarre P. J., 2015, *MNRAS*, 453, 3912
 Massey P., Thompson A. B., 1991, *AJ*, 101, 1408
 Merrill P. W., 1934, *PASP*, 46, 206
 Milisavljevic D., et al., 2014, *ApJ*, 782, L5
 Mink D. J., 2011, in Evans I. N., Accomazzi A., Mink D. J., Rots A. H., eds, *Astronomical Society of the Pacific Conference Series Vol. 442*, *Astronomical Data Analysis Software and Systems XX*. p. 305
 Miroshnichenko A. S., Chentsov E. L., Klochkova V. G., 2000, *A&AS*, 144, 379
 Moffat A. F. J., Drissen L., Lamontagne R., Robert C., 1988, *ApJ*, 334, 1038
 Morton D. C., Smith W. H., 1973, *ApJS*, 26, 333
 Oka T., Welty D. E., Johnson S., York D. G., Dahlstrom J., Hobbs L. M., 2013, *Astrophys. J.*, 773, 42
 Panov K. P., Seggewiss W., 1990, *A&A*, 227, 117
 Sarre P. J., 2006, *Journal of Molecular Spectroscopy*, 238, 1
 Sarre P. J., Miles J. R., Kerr T. H., Hibbins R. E., Fossey S. J., Somerville W. B., 1995, *MNRAS*, 277, L41
 Saurin T. A., Bica E., Bonatto C., 2010, *MNRAS*, 407, 133
 Seab C., 1995, in Tielens A. G. G. M., Snow T. P., eds, *Astrophysics and Space Science Library Vol. 202*, *The Diffuse Interstellar Bands*. p. 129, doi:10.1007/978-94-011-0373-2_14
 Skinner S. L., Zhekov S. A., Güdel M., Schmutz W., 2015, *ApJ*, 799, 124
 Smith K. T., Fossey S. J., Cordiner M. A., Sarre P. J., Smith A. M., Bell T. A., Viti S., 2013, *MNRAS*, 429, 939

- Szentgyorgyi A. H., Furész G., 2007, in Kurtz S., ed., *Revista Mexicana de Astronomia y Astrofisica Conference Series Vol. 28*, *Revista Mexicana de Astronomia y Astrofisica Conference Series*. pp 129–133
- Tuthill P. G., Monnier J. D., Danchi W. C., 1999, *Nature*, 398, 487
- Underhill A. B., Gilroy K. K., Hill G. M., 1990, *ApJ*, 351, 651
- Walborn N. R., Fitzpatrick E. L., 2000, *PASP*, 112, 50
- Weselak T., Galazutdinov G. A., Han I., Krelowski J., 2010, *MNRAS*, 401, 1308
- Wright N. J., Drew J. E., Mohr-Smith M., 2015, *MNRAS*, 449, 741
- van der Hucht K. A., 2001, *New Astron. Rev.*, 45, 135

This paper has been typeset from a $\text{\TeX}/\text{\LaTeX}$ file prepared by the author.